Journal of Power Sources 195 (2010) 1589–1593

Contents lists available at ScienceDirect

Journal of Power Sources

journal homepage: www.elsevier.com/locate/jpowsour

Short communication

Study of ethanol electro-oxidation in acid environment on Pt_3Sn/C anode catalysts prepared by a modified polymeric precursor method under controlled synthesis conditions

R.F.B. De Souza[a], L.S. Parreira[a], D.C. Rascio[a], J.C.M. Silva[a], E. Teixeira-Neto[a], M.L. Calegaro[b], E.V. Spinace[c], A.O. Neto[c], M.C. Santos[a,*]

[a] LEMN – Laboratório de Eletroquímica e Materiais Nanoestruturados, CCNH – Centro de Ciências Naturais e Humanas, UFABC – Universidade Federal do ABC, CEP 09.210-170, Rua Santa Adélia 166, Bairro Bangu, Santo André, SP, Brazil
[b] Grupo de Materiais Eletroquímicos e Métodos Eletroanalíticos, Instituto de Química de São Carlos, Universidade de São Paulo, Caixa Postal 780, 13566-590 São Carlos, SP, Brazil
[c] Instituto de Pesquisas Energéticas e Nucleares, IPEN, CNEN/SP, Av. Prof. Lineu Prestes, 2242 Cidade Universitária, CEP 05508-900, São Paulo, SP, Brazil

ARTICLE INFO

Article history:
Received 6 August 2009
Received in revised form
20 September 2009
Accepted 30 September 2009
Available online 9 October 2009

Keywords:
Ethanol oxidation reaction
Electrocatalysis
Platinum–tin alloys
Nanoparticles
Polymeric precursor method

ABSTRACT

A carbon-supported binary Pt_3Sn catalyst has been prepared using a modified polymeric precursor method under controlled synthesis conditions. This material was characterized using X-ray diffraction (XRD), and the results indicate that 23% (of a possible 25%) of Sn is alloyed with Pt, forming a dominant Pt_3Sn phase. Transmission electron microscopy (TEM) shows good dispersion of the electrocatalyst and small particle sizes (3.6 nm ± 1 nm). The polarization curves for a direct ethanol fuel cell using Pt_3Sn/C as the anode demonstrated improved performance compared to that of a PtSn/C E-TEK, especially in the intrinsic resistance-controlled and mass transfer regions. This behavior is probably associated with the Pt_3Sn phase. The maximum power density for the Pt_3Sn/C electrocatalyst (58 mW cm^{-2}) is nearly twice that of a PtSn/C E-TEK electrocatalyst (33 mW cm^{-2}). This behavior is attributed to the presence of a mixed Pt_9Sn and Pt_3Sn alloy phase in the commercial catalysts.

1. Introduction

Fuel cells [1] are widely recognized as attractive devices for the production of electric energy via combustion of a chemical product. Low temperature fuel cells, which are generally designed around a proton electrolyte membrane, have shown potential in a broad range of power applications. Alcohols (especially methanol) have widely been proposed as possible fuels in portable fuel cells, such as those that would be used to power electric vehicles [2,3].

Ethanol is an attractive fuel for low temperature fuel cells because it can be produced in large quantities from agricultural products or other biomass, as well as because it is less toxic than methanol. In addition, ethanol has a higher theoretical mass energy density (8.01 kW h kg^{-1}) than methanol (6.09 kW h kg^{-1}) [4]. In contrast, complete oxidation of ethanol to CO_2 is more complicated than complete oxidation of methanol due to the strength of C–C bonds and the formation of CO-intermediates that can poison the anode catalysts (Pt or Pt-based alloys) by generating acetic acid during the oxidation process [5–7]. Thus, much modern-day research examining the oxidation of small organic molecules has focused on the development of new electrocatalytic materials [1] and new methods of catalyst preparation [6]. New methods of catalyst preparation are key in defining the activity of the final product because several important parameters, such as the electroactive area, the chemical nature of the surface, the morphology, and the ability to control the formation of secondary phases, are directly related to the catalyst preparation methodology.

Binary Pt–Ru and Pt–Sn have been extensively investigated as anode materials for direct ethanol fuel cells (DEFCs), as have the related ternary Pt–Ru-based and Pt–Sn-based catalysts [1]. As in the case of methanol oxidation, the superior performance of these binary and ternary electrocatalysts for ethanol oxidation, when compared to Pt alone, has been attributed to the bifunctional effect (promoted mechanism) [8,9] and to electronic interactions between Pt and the alloyed metals (intrinsic mechanism) [8,10,11]. In contrast to the case of methanol oxidation, the best binary catalyst for ethanol oxidation in an acidic medium is Pt–Sn rather than Pt–Ru [1]. As a result, it is reasonable that research and development of new catalysts for ethanol oxidation in acidic environments should focus on this system. As noted above, special attention must be given to the experimental method selected to prepare the catalyst.

* Corresponding author. Tel.: +55 11 4996 0163; fax: +55 11 4437 8350.
E-mail address: mauro.santos@ufabc.edu.br (M.C. Santos).

0378-7753/$ – see front matter © 2009 Elsevier B.V. All rights reserved.
doi:10.1016/j.jpowsour.2009.09.065

The promoting effect of Sn on the activity of Pt catalysts has been comprehensively analyzed by Antolini [1], who reviewed the most relevant research examining various aspects of catalysts for ethanol oxidation. Based on this review and other related works [12–14], it is clear that the optimum Sn content in a binary Pt–Sn catalyst system has yet to be determined, and that the optimal ratio appears to depend on both cell temperature and the ratio of alloyed and non-alloyed tin. A DEFC using Pt_3Sn as the anode catalyst shows the best average performance in the temperature range from 70 to 100 °C, as reported by Colmati et al. [15].

In analyzing various reports that describe methods to prepare binary Pt–Sn catalysts, it seems that production of Pt_3Sn as a pure and exclusive phase rarely occurs regardless of the synthetic procedure. Extensive investigations performed by Lamy [16–19] and Xin [20–23], for example, studied ethanol oxidation on carbon-supported Pt–Sn prepared by different methods, including the co-impregnation reduction method [16,17], the "Bonneman" method [18,19] and a modified polyol method [20–23]. In all these cases, the majority of Sn in the catalysts as prepared existed in an oxidized, non-alloyed state. The formic acid method has been widely used by Gonzalez et al. to investigate the Pt–Sn system [24–27]. As prepared, the synthesized Pt–Sn catalysts demonstrated a low degree of alloy formation and high Sn oxide content [27]. When thermally treated, the extent of Sn alloying in the catalysts increased [25,26]. In addition, various alloy phases were produced depending on the Pt/Sn atomic ratio of the catalysts.

The aim of this work was to use a modified polymeric precursor method (PPM) developed by De Souza et al. [28] to produce Pt_3Sn/C, which is recognized as one of the best electrocatalysts for the ethanol oxidation reaction (EOR). This electrocatalyst has been characterized using X-ray diffraction and transmission electron microscopy, and its performance has been evaluated using polarization and density power curves.

2. Materials and methods

Pt_3Sn (20% w/w) on carbon XC72 electrocatalyst was prepared using a modified polymeric precursor method (PPM) [28]. For this purpose, a mass ratio of 1:50:400 (metallic precursor:citric acid (CA):ethylene glycol (EG)) was used to prepare the polymeric resin. Chloroplatinic acid ($H_2PtCl_6{\cdot}6H_20$, Sigma–Aldrich) and tin chloride ($SnCl_2{\cdot}2H_20$, Merck) were used as the metallic precursors. The prepared polymeric resin was stored under refrigeration. The catalyst was prepared by placing a pre-determined volume of resin in an appropriate amount of carbon Vulcan XC-72 (Cabot Corporation), followed by the addition of enough EG to cover the carbon powder. The pre-determined volume of resin was chosen to yield a final product containing Pt and Sn in an atomic ratio of 3:1. The mixture was homogenized in an ultrasonic bath for over 60 min and then thermally treated at 400 °C for 2 h in a N_2 atmosphere after evaporation of the excess solvent.

As mentioned above, the present experimental procedure is based on PPM [28], with the goal of producing Pt_3Sn/C that is free of secondary alloy phases. A large excess of EG was used to enhance dispersion of the carbon support, providing an improved environment for the production of a catalyst with a high surface area. This increased surface area is due to better contact between the carbon powder and the stable metallic precursors pre-formed in solution by complexation of tin chloride or chloroplatinic acid and CA. One of the main advantages of the PPM approach is its ability to effectively mix different metal ions when they are combined [29], thereby yielding a product with a well-defined composition. In PPM, this is achieved by reacting the metal precursors with citric acid to form stable metal–chelate complexes, which are then immobilized in a rigid organic polymer network. As a result, segregation of the various precursors during high-temperature polymer decomposition is avoided. Based on the above advantages, the PPM was used to prepare a catalyst presenting a specific configuration (Pt_3Sn/C). It must be emphasized that this procedure is normally used to combine two or more organo-metallic precursors to produce mixed metal oxides that can be used for different purposes. Thus, appropriate choice of the final synthesis and thermal treatment conditions is essential to avoid or to minimize the production of metal oxides. The use of atmospheres containing oxygen must be avoided because they will contribute to the production of metal oxides [30]. For this reason, the thermal treatment was conducted in an inert nitrogen atmosphere at 400 °C. This is the minimum temperature value necessary for the complete degradation of the polymeric resin. Under such conditions and in the presence of carbon, the amount of oxidized species in the catalysts can be decreased [31]. The carbon substrate used to support the catalyst particles also acts as a reducing agent at sufficiently high temperatures. Using higher temperatures causes two collateral undesirable effects: the agglomeration of the metallic particles, decreasing the catalyst surface area, and the formation of metal carbides.

XRD analyses were performed using a Rigaku diffractometer (model Multiflex) with a Cu Kα radiation source. Morphological information for the catalysts was obtained via TEM using a JEOL JEM 2100 microscope operating at 200 kV. The samples were prepared by ultrasonically treating the catalyst powders in isopropanol. A drop of the resulting dispersion was placed on thin carbon films deposited on standard TEM copper grids and dried in air.

To test the activity during ethanol oxidation, Pt_3Sn/C PPM or PtSn/C E-TEK (for comparison purposes) with a Pt/Sn stoichiometry of 1:1 and a metal loading of 20 wt.% was used as the anode; 20 wt.% Pt/C E-TEK was used as the cathode in the gas diffusion electrodes of single unit fuel cells. The diffusion layer consisted of carbon powder (Vulcan XC-72, Cabot) with 15% (w/w) polytetrafluorethylene (PTFE, TE-306A, DuPont) deposited onto a carbon cloth substrate (E-TEK). The electrocatalyst was deposited on top of this layer in the form of a homogeneous dispersion made with Nafion® solution (5 wt.%, Aldrich) and isopropanol (J.T. Baker). All electrodes contained 1 mg Pt cm^{-2} in the anode or the cathode. After preparation, the electrodes were hot pressed on both sides of a Nafion® 117 membrane at 100 °C for 2 min under a pressure of 225 kgf cm^{-2}. Prior to use, the membranes were exposed to 3 wt.% H_2O_2, washed thoroughly with distilled water and treated with 0.5 mol L^{-1} H_2SO_4. The performance of the ethanol fuel cell containing each catalyst was determined in a single cell with a geometric area of 5 cm^2. The temperature was set to 100 °C for the fuel cell and 80 °C for the oxygen humidifier. The fuel (2 mol L^{-1} ethanol aqueous solutions) was delivered at approximately 2 mL min^{-1}, and the oxygen flow was set to 500 mL min^{-1} and a pressure of 2 bar. Polarization curves were obtained using a TDI RBL 488 electronic load.

3. Results and discussion

Fig. 1 shows histograms and TEM images for Pt_3Sn/C PPM (Fig. 1a and b) and PtSn/C E-TEK (Fig. 1c and d). The electrocatalysts were well distributed on the carbon support, with particle sizes between 3–4 nm and 2–3 nm, respectively. The primary difference in the particle sizes is that the commercial material was better dispersed on the carbon support than the Pt_3Sn/C PPM prepared in our laboratory. It is important to point out that 100% of the particles are between 0 and 10 nm in size. Table 1 gives the maximum and minimum diameters of the particles, along with the mean deviation. This result is in good agreement with the work of Purgato et al. [30], in which platinum–tin catalysts were prepared by a method similar to that used in the present work.

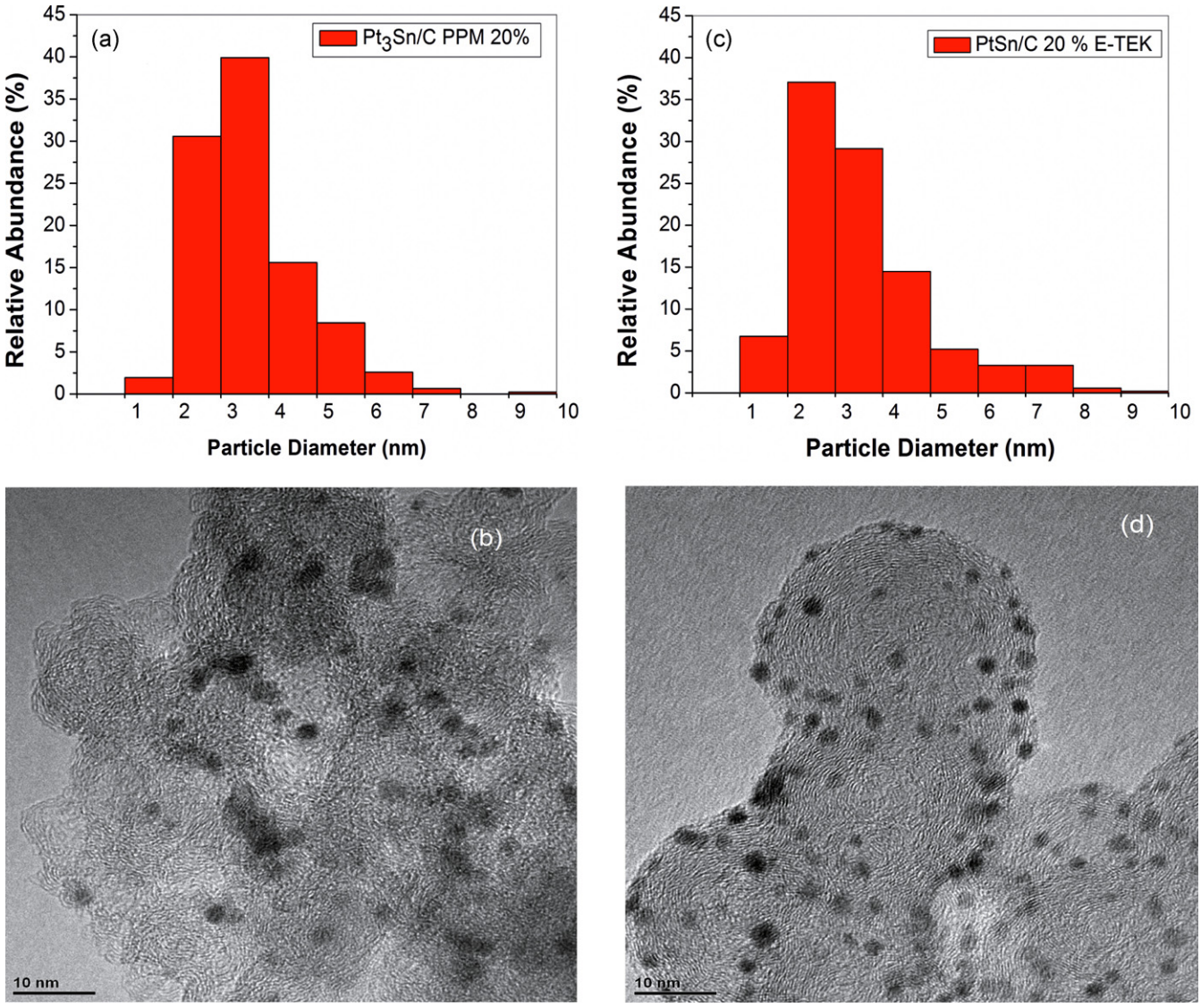

Fig. 1. (a) Histogram of catalyst particle mean diameter distribution over the size range from 0 to 10 nm for 20 wt.% Pt_3Sn/C PPM in the left column; (b) TEM micrograph of this electrocatalyst on the right; (c) histogram of catalyst particle mean diameter distribution over the size range from 0 to 10 nm for PtSn/C E-TEK 20% in the left column; and (d) TEM micrograph of this electrocatalyst in the right.

Fig. 2 shows the XRD diffractograms of the as-prepared Pt_3Sn/C PPM alloy catalyst. The diffraction peak at 20–25° is attributed to the (0 0 2) plane of the hexagonal phase of Vulcan XC-72 carbon. The XRD pattern of the as-prepared Pt_3Sn/C PPM shows peaks that are characteristic of face-centered cubic (fcc) crystalline Pt. These diffraction peaks are shifted to slightly lower 2θ degrees than the corresponding peaks of a pure Pt catalyst, suggesting lattice expansion due to the presence of larger Sn atoms. This finding is consistent with alloy formation between Pt and Sn. Table 2 summarizes various parameters obtained for the Pt_3Sn/C PPM alloy catalyst based on the XRD data in Fig. 2, including the diffraction angles, the corresponding diffraction planes, the *d*-spacings (d_{hkl}) of the reflecting planes (calculated based on the Bragg equa-

Table 1
Morphological information obtained from TEM images of the investigated catalysts.

Electrocatalyst	Mean diameter (nm)	Standard deviation (nm)	Maximum diameter (nm)	Minimum diameter (nm)
Pt_3Sn/C PPM	3.6	1.1	9.9	1.7
PtSn/C E-TEK	3.5	1.4	9.9	1.4

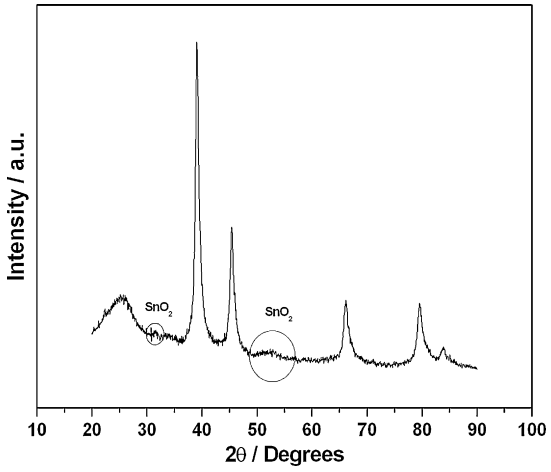

Fig. 2. X-ray diffraction (XRD) spectra of 20 wt.% Pt_3Sn/C PPM.

Table 2
Structural parameters of Pt_3Sn/C PPM obtained from the XRD experiments.

2θ (°)	Crystal plane	Network parameter a_{exp} (Å)	d_{hkl} (Å)
39.12	(1 1 1)	3.9854	2.3010
45.46	(2 0 0)	3.9882	1.9941
66.20	(2 2 0)	3.9901	1.4107
79.62	(3 1 1)	3.9909	1.2033
83.88	(2 2 2)	3.9924	1.1525

tion) and the network parameter a_{exp}. The network parameter was calculated from the following expression for the cubic system [32]:

$$a_{exp} = d_{hkl}\sqrt{h^2 + k^2 + l^2} \quad (1)$$

where h, k and l are the indices of the planes.

The lattice parameter determined from this equation for each diffraction plane is between 3.9854 and 3.9924 Å. The values obtained by this procedure are generally lower than those of the corresponding bulk material. This effect may be attributed to lattice contraction [33]. To obtain the true value of the lattice constant, an extrapolation procedure was used in which the calculated lattice constants were plotted against an error function x defined as [34,35]:

$$x = \frac{1}{2}\left(\frac{\cos^2\theta}{\sin\theta} + \frac{\cos^2\theta}{\theta}\right) \quad (2)$$

where θ is the Bragg angle (expressed in radians).

Fig. 3 shows the plot of a_{exp} versus x for the lattice parameters calculated based on the peak positions of each diffraction plane of Pt_3Sn/C PPM. The plane associated with the Vulcan XC-72 carbon is ignored in these calculations, as it is not related to the catalyst itself. Extrapolation to $x = 0$ yields the true network parameter, a_c. A value of $a_c = 3.9944$ Å was obtained for the true lattice parameter, which is very close to the value expected for a Pt_3Sn alloy phase (4.0015 Å). This result indicates that almost all the Sn originally used in the synthesis is alloyed with Pt, forming Pt_3Sn/C. Following a procedure described by Colmati et al. [24], the amount of alloyed Sn (f_{Sn}) in the Pt_3Sn/C PPM catalyst can be calculated using the relationship:

$$f_{Sn} = \left[\frac{(a_c - a_o)}{(a_s - a_o)}\right] x_s \quad (3)$$

where a_c is the experimental lattice parameter calculated above, $a_o = 3.9075$ Å [36] is the lattice parameter of a Pt/C material with size (~4.5 nm) comparable to the size of the catalyst particles in the

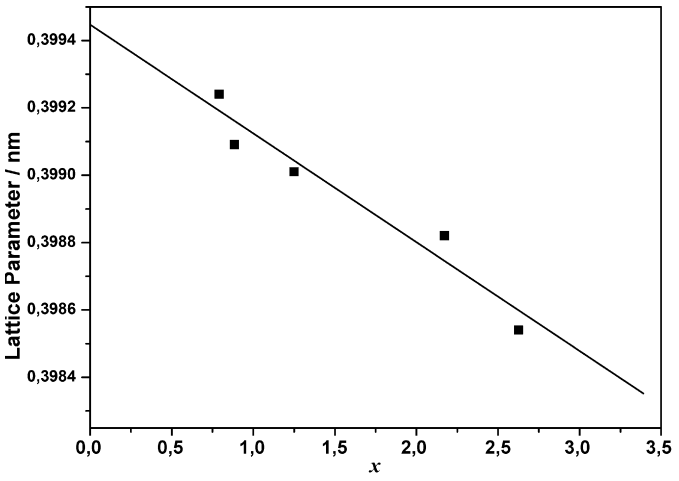

Fig. 3. Nelson–Riley plot of the lattice parameter for 20 wt.% Pt_3Sn/C PPM electrocatalyst.

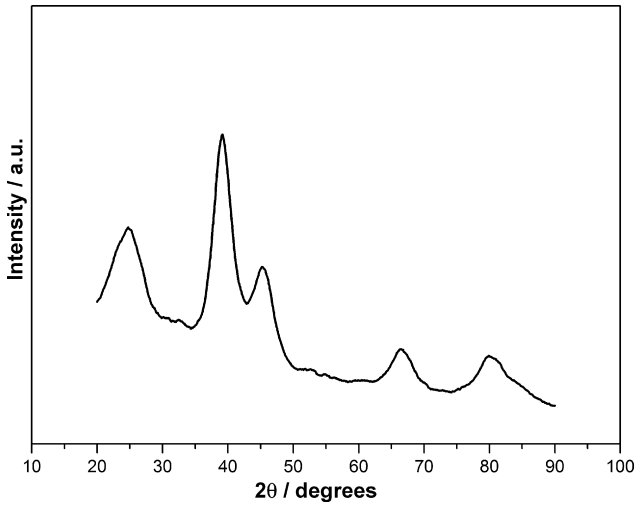

Fig. 4. XRD diffractograms of 20 wt.% PtSn/C E-TEK electrocatalyst.

present work, a_s is the network parameter for Pt_3Sn/C (4.0015 Å, ca. 100% alloyed [37]), and x_s is the Sn atomic fraction (0.25). Substituting the respective values into equation (3) yields a value of 0.23 for f_{Sn}, indicating that 23% out of the 25% mass fraction is present as Pt_3Sn/C The remainder is probably present as amorphous tin oxide, as suggested by the small peaks at 34° and 52° in Fig. 2 [7].

The findings above indicate that the PPM approach can be used to produce almost exclusively Pt_3Sn/C (>90%) if the synthesis conditions are well-controlled. This conclusion is further supported if the results of this research are compared with similar work that was performed using the same method, but in different conditions, to prepare carbon-supported Pt–Sn catalysts [30]. In that research, different experimental conditions resulted in different compositions.

Fig. 4 provides the XRD patterns of PtSn/C E-TEK catalyst. As in the case of Pt_3Sn/C PPM, the profile shows the characteristic peaks of crystalline Pt with fcc structure, but at lower angles than are seen for pure Pt. This result indicates alloy formation between Sn and Pt. The presence of two small, broad peaks near 34° and 52° indicates that a small amount of SnO_2 is also produced in this case. By using the same procedure as described above to calculate the network parameter (not shown), a value of 3.9825 Å was found. This value is very close to the value of 3.9880 Å calculated by Radmilovic et al. [38] for a commercial carbon-supported Pt–Sn catalyst with a mass ratio of 1.23:1. Radmilovic et al. [38] attributed this value to a mixture of near-stoichiometric Pt_3Sn ($a_o = 3.9880$ Å) and stoichiometric PtSn along with SnO_2.

Fig. 5a shows the performance of direct ethanol fuel cells with Pt_3Sn/C PPM and commercial (E-TEK) carbon-supported Pt–Sn as the anode catalysts. In Fig. 5a, although the open circuit voltage (0.71 V) of the fuel cell containing Pt_3Sn/C PPM electrocatalyst is slightly lower than the corresponding value for PtSn/C E-TEK (0.77 V), the single cell with Pt_3Sn/C as the anode catalyst exhibits better overall performance than that equipped with PtSn/C E-TEK, especially in the intrinsic resistance-controlled region and the mass transfer region. The particular performance observed for each material is certainly related to the differences that exist in each structure. In particular, the lower proportion of the Pt_3Sn/C alloy phase in the commercial catalyst is expected to be significant. On the basis of work by Colmati et al. [24] studying the electro-oxidation of ethanol on different Pt–Sn alloys prepared by the formic acid method, it was concluded that the activity of Pt–Sn catalysts seems to be dependent on the amounts of alloyed and non-alloyed Sn. In addition, it was determined that the activity of Pt_3Sn is higher than that of other Pt–Sn alloy phases in the EOR. This

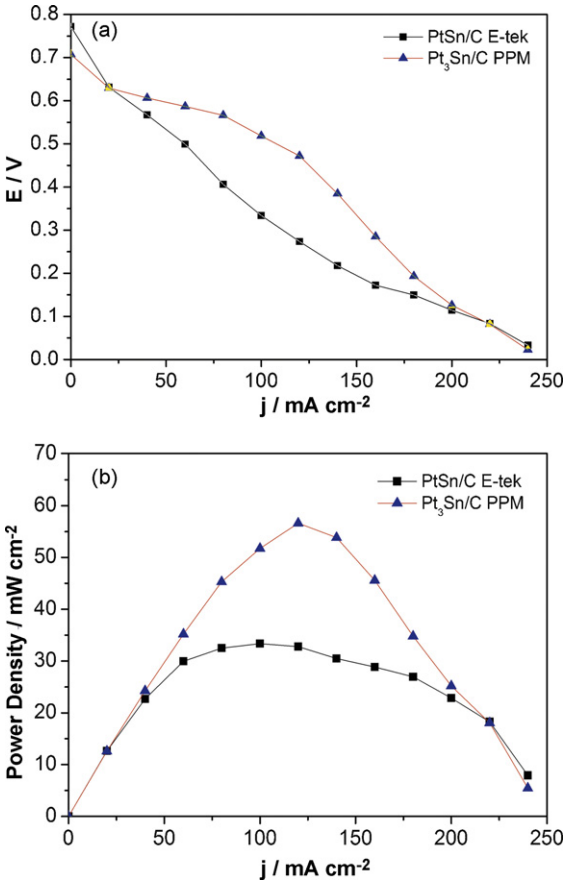

Fig. 5. Polarization curves (a) and power density curves (b) in 5 cm^2 DEFC at 100 °C using 20 wt.% Pt_3Sn/C PPM or 20 wt.% PtSn/C E-TEK as anode catalysts (1 mg Pt cm^{-2}) and 20 wt.% Pt/C E-TEK as the cathode catalyst (1 mg Pt cm^{-2}). Nafion® 117 was used as the membrane.

conclusion agrees with the results of the present work. The Pt_3Sn/C PPM is composed almost entirely of a Pt_3Sn alloy phase and a small amount of SnO_2. The PtSn/C commercial catalyst is composed of a mixture of Pt_3Sn, PtSn, and also a small amount of amorphous SnO_2. Thus, the better performance of the Pt_3Sn/C PPM for ethanol oxidation is due to a higher proportion of Pt_3Sn than in the commercial catalyst.

The power density curve presented in Fig. 5b corroborates the results presented in Fig. 5a, and it further shows that the maximum power density obtained for the Pt_3Sn/C PPM (58 mW cm^{-2}) is almost twice that obtained for the commercial PtSn/C E-TEK catalyst (33 mW cm^{-2}). The development of an experimental methodology for the production of Pt–Sn catalysts with a single alloy phase has interesting implications for the development of catalysts for the EOR in acidic environments. The ethanol oxidation reaction is a very complicated process that may be more conveniently studied in catalytic systems where the structure and composition can be more easily and cleanly defined. The synthetic methodology used in the present work was systematically studied for the considered composition (Pt_3Sn), and very reproducible results were obtained, showing that this experimental procedure, when conducted under very specific experimental conditions, can provide an excellent degree of control for such studies.

4. Conclusions

The TEM and XRD results demonstrate that Pt_3Sn/C catalysts with low metal loadings (20% on carbon) can be easily prepared with small particle sizes via a modified polymeric precursor method if controlled synthesis conditions are used. This electrocatalyst yielded superior activity to that of the commercial PtSn/C material E-TEK for ethanol oxidation in a DEFC. This behavior was attributed to the presence of a mixed alloy phase composed of Pt_9Sn and Pt_3Sn in the commercial catalyst. Since Pt_9Sn is less active in the EOR than Pt_3Sn, a lower mean performance was observed for the commercial catalyst across all potential regions.

Acknowledgements

The authors wish to thank the Brazilian Funding Institutions (CNPq (Process Number: 474742/2008-8), CAPES, and FAPESP (Processes Numbers: 05/59992-6, 08/58789-0, 08/58788-4)) and UFABC for their financial support. Erico Teixeira Neto thanks LME-LNLS for the use of the JEOL JEM 2100 TEM-MSC microscope.

References

[1] E. Antolini, J. Power Sources 170 (2007) 1–12.
[2] C. Lamy, E.M. Belgsir, J.M. Leger, J. Appl. Electrochem. 31 (2001) 799–809.
[3] E. Peled, T. Duvdevani, A. Aharon, A. Melman, Electrochem. Solid State Lett. 4 (2001) A38–A41.
[4] F. Delime, J.M. Leger, C. Lamy, J. Appl. Electrochem. 28 (1998) 27–35.
[5] S.Q. Song, W.J. Zhou, Z.H. Zhou, L.H. Jiang, G.Q. Sun, Q. Xin, V. Leontidis, S. Kontou, P. Tsiakaras, Int. J. Hydrogen Energy 30 (2005) 995–1001.
[6] C. Coutanceau, S. Brimaud, C. Lamy, J.M. Leger, L. Dubau, S. Rousseau, F. Vigier, Electrochim. Acta 53 (2008) 6865–6880.
[7] A.O. Neto, L.A. Farias, R.R. Dias, M. Brandalise, M. Linardi, E.V. Spinace, Electrochem. Commun. 10 (2008) 1315–1317.
[8] N.M. Markovic, H.A. Gasteiger, P.N. Ross, X. Jiang, I. Villegas, M.J. Weaver, Electrochim. Acta 40 (1995) 91–98.
[9] S.L. Gojkovic, T.R. Vidakovic, D.R. Durovic, Electrochim. Acta 48 (2003) 3607–3614.
[10] T. Iwasita, Electrochim. Acta 47 (2002) 3663–3674.
[11] P.A. Christensen, A. Hamnett, G.L. Troughton, J. Electroanal. Chem. 362 (1993) 207–218.
[12] M. Zhu, G. Sun, Q. Xin, Electrochim. Acta 54 (2009) 1511–1518.
[13] R. Alcala, J.W. Shabaker, G.W. Huber, M.A. Sanchez-Castillo, J.A. Dumesic, J. Phys. Chem. B 109 (2005) 2074–2085.
[14] X.L. Tang, B.C. Zhang, Y. Li, Y. Xu, Q. Xin, W.J. Shen, J. Mol. Catal. A 235 (2005) 122–129.
[15] F. Colmati, E. Antolini, E.R. Gonzalez, Electrochim. Acta 50 (2005) 5496–5503.
[16] F. Vigier, C. Coutanceau, A. Perrard, E.M. Belgsir, C. Lamy, J. Appl. Electrochem. 34 (2004) 439–446.
[17] F. Vigier, C. Coutanceau, F. Hahn, E.M. Belgsir, C. Lamy, J. Electroanal. Chem. 563 (2004) 81–89.
[18] C. Lamy, S. Rousseau, E.M. Belgsir, C. Coutanceau, J.M. Leger, Electrochim. Acta 49 (2004) 3901–3908.
[19] J.M. Leger, S. Rousseau, C. Coutanceau, F. Hahn, C. Lamy, Electrochim. Acta 50 (2005) 5118–5125.
[20] W. Zhou, Z. Zhou, S. Song, W. Li, G. Sun, P. Tsiakaras, Q. Xin, Appl. Catal. B 46 (2003) 273–285.
[21] L. Jiang, G. Sun, Z. Zhou, W. Zhou, Q. Xin, Catal. Today 93–95 (2004) 665–670.
[22] W.J. Zhou, S.Q. Song, W.Z. Li, G.Q. Sun, Q. Xin, S. Kontou, K. Poulianitis, P. Tsiakaras, Solid State Ionics 175 (2004) 797–803.
[23] L. Jiang, G. Sun, S. Sun, J. Liu, S. Tang, H. Li, B. Zhou, Q. Xin, Electrochim. Acta 50 (2005) 5384–5389.
[24] F. Colmati, E. Antolini, E.R. Gonzalez, J. Electrochem. Soc. 154 (2007) B39–B47.
[25] F. Colmati, E. Antolini, E.R. Gonzalez, Appl. Catal. B 73 (2007) 106–115.
[26] F. Colmati, E. Antolini, E.R. Gonzalez, J. Solid State Electrochem. 12 (2008) 591–599.
[27] F. Colmati, E. Antolini, E.R. Gonzalez, J. Power Sources 157 (2006) 98–103.
[28] R.F.B. De Souza, A.E.A. Flausino, D.C. Rascio, R.T.S. Oliveira, E.T. Neto, M.L. Calegaro, M.C. Santos, Appl. Catal. B 91 (2009) 516–523.
[29] M. Kakihana, J. Sol–Gel Sci. Technol. 6 (1996) 7–55.
[30] F.L.S. Purgato, P. Olivi, J.M. Leger, A.R. de Andrade, G. Tremiliosi-Filho, E.R. Gonzalez, C. Lamy, K.B. Kokoh, J. Electroanal. Chem. 628 (2009) 81–89.
[31] H.Q. Li, G.Q. Sun, Y. Gaot, Q. Jiang, Z. Jia, Q. Xin, J. Phys. Chem. C 111 (2007) 15192–15200.
[32] M.A. Ahmed, A. Tawfik, M.K. Elnimr, A.A. Elhasab, J. Mater. Sci. Lett. 10 (1991) 549–551.
[33] F.C. Eze, Mater. Chem. Phys. 89 (2005) 205–210.
[34] H.P. Klug, L.E. Alexander, X-ray Diffraction Procedures for Polycrystalline and Amorphous Materials, Wiley, New York, 1974.
[35] J.B. Nelson, D.P. Riley, Proc. Phys. Soc. (Lond.) 57 (1945) 160–177.
[36] J.R.C. Salgado, E.R. Gonzalez, Eclet. Quim. 28 (2003) 77–85.
[37] M. Hoheisel, S. Speller, J. Kuntze, A. Atrei, U. Bardi, W. Heiland, Phys. Rev. B 63 (2001) 245403.
[38] V. Radmilovic, T.J. Richardson, S.J. Chen, P.N. Ross Jr., J. Catal. 232 (2005) 199–209.